Abstracta

Ano XV - N. 03

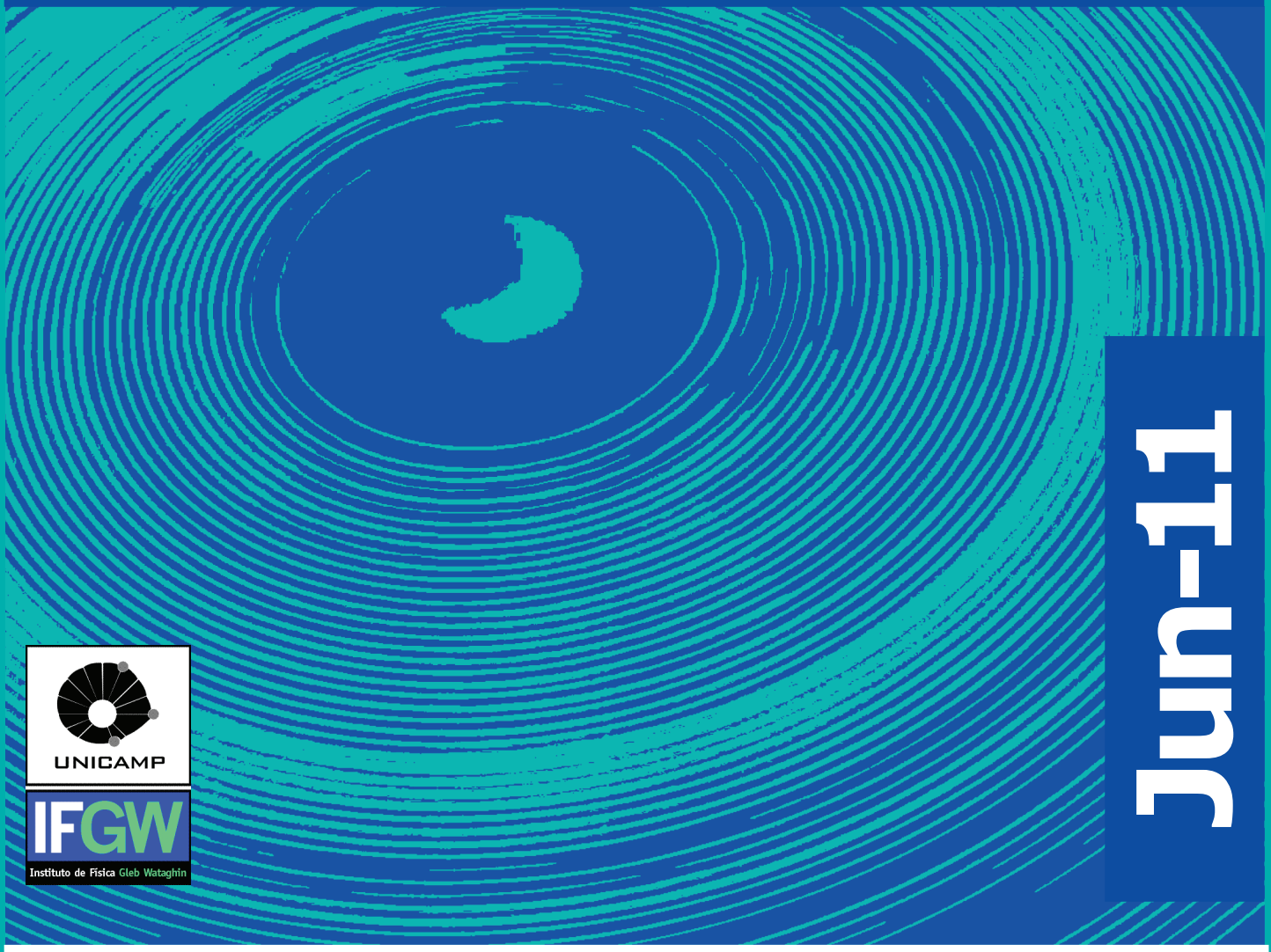

Jun-11

UNICAMP

IFGW

Instituto de Física Gleb Wataghin

Trabalhos Publicados

Maio 2011 à Junho 2011

P070-11 à P102 -11

Trabalhos Publicados

[P070-11] "Advanced functionality for radio analysis in the Offline software framework of the Pierre Auger Observatory"

Abreu, P., Aglietta, M., Ahn, E. J., Albuquerque, I. F. M., Allard, D., Allekotte, I., Allen, J., Allison, P., Castillo, J., Alvarez-Muniz, J., Ambrosio, M., Aminaei, A., Anchordoqui, L., Andringa, S., Anticic, T., Aramo, C., Arganda, E., Arqueros, F., Asorey, H., et all

The advent of the Auger Engineering Radio Array (AERA) necessitates the development of a powerful framework for the analysis of radio measurements of cosmic ray air showers. As AERA performs "radio-hybrid" measurements of air shower radio emission in coincidence with the surface particle detectors and fluorescence telescopes of the Pierre Auger Observatory, the radio analysis functionality had to be incorporated in the existing hybrid analysis solutions for fluorescence and surface detector data. This goal has been achieved in a natural way by extending the existing Auger Offline software framework with radio functionality. In this article, we lay out the design, highlights and features of the radio extension implemented in the Auger Offline framework. Its functionality has achieved a high degree of sophistication and offers advanced features such as vectorial reconstruction of the electric field, advanced signal processing algorithms, a transparent and efficient handling of FFTs, a very detailed simulation of detector effects, and the read-in of multiple data formats including data from various radio simulation codes. The source code of this radio functionality can be made available to interested parties on request. (C) 2011 Elsevier B.V. All rights reserved

Nuclear Instruments & Methods in Physics Research Section A-Accelerators Spectrometers Detectors and Associated Equipment 635[1], 92-102. 2011.

[P071-11] "An effective method to probe local magnetostatic properties in a nanometric FePd antidot array"

Beron, F., Pirota, K. R., Vega, V., Prida, V. M., Fernandez, A., Hernando, B., and Knobel, M.

A simple method to quantitatively characterize the local magnetic behaviour of a patterned nanostructure, like a ferromagnetic thin film of antidot arrays, is proposed. The first-order reversal curve (FORC) analysis, coupled with simulations using physically meaningful hysterons, allows us to obtain a quantitative and physically related description of the interaction field and each magnetization reversal process. The hysterons system is built from previously known hypotheses on the magnetic behaviour of the sample. This method was successfully applied to a highly hexagonal ordered FePd antidot array with nanometric dimensions. We achieved a complete characterization of the two different magnetization reversal mechanisms in function of the in-plane applied field angle. For a narrow range of high fields, the magnetization initiates rotating reversibly around the pores, while at lower fields, domain walls are nucleated and propagated. This in-plane magnetization reversal mechanism, partly reversible and partly irreversible, is the only angularly dependent one. While going away from the easy axis, its reversible proportion increases, as well as its switching field distribution. Finally, the results indicate that the high surface roughness between adjacent holes of the antidot thin film induces a parallel interaction field. The proposed method demonstrates its ability also to be applied to characterizing patterned nanostructures with rather complex magnetization reversal processes

New Journal of Physics 13. 013035. 2011.

[P072-11] "Charged Brownian particles: Kramers and Smoluchowski equations and the hydrothermodynamical picture"

Lagos, R. E. and Simoes, T. P.

We consider a charged Brownian gas under the influence of external and non-uniform electric, magnetic and mechanical fields, immersed in a non-uniform bath temperature. With the collision time as an expansion parameter, we study the solution to the associated Kramers equation, including a linear reactive term. To the first order we obtain the asymptotic (overdamped) regime, governed by transport equations, namely: for the particle density, a Smoluchowski-reactive like equation; for the particle's momentum density, a generalized Ohm's-like equation; and for the particle's energy density, a Maxwell-Cattaneo-like equation. Defining a nonequilibrium temperature as the mean kinetic energy density, and introducing Boltzmann's entropy density via the one particle distribution function, we present a complete thermohydrodynamical picture for a charged Brownian gas. We probe the validity of the local equilibrium approximation. Onsager relations, variational principles associated to the entropy production, and apply our results to: carrier transport in semiconductors, hot carriers and Brownian motors. Finally, we outline a method to incorporate non-linear reactive kinetics and a mean field approach to interacting Brownian particles. (C) 2011 Elsevier B.V. All rights reserved

Physica A-Statistical Mechanics and Its Applications 390[9], 1591-1601. 2011.

[P073-11] "Cu induced coercivity enhancement in the low viscosity GdCo5-xCux system"

de Oliveira, L. A. S., Sinnecker, J. P., Grossinger, R., Penton-Madrigal, A., and Estevez-Rams, E.

We investigate the influence of Cu substitution, on the coercivity and magnetic viscosity, in the ternary system GdCo5-xCux (x = 0, 0.5, 1, 1.5, 2 and 2.5) with different field sweep rates. All samples have been studied in the as cast state and crystallize in a single phase CaCu5 structure. With Cu addition, the coercivity was 10 times enhanced for x = 1.5. The behavior of the coercivity H-c against field sweep rate, dH/dt, shows that the GdCo5-xCux system exhibits only a small magnetic viscosity effect, a desirable property for magnetic dynamic applications under high magnetic field. (c) 2011 Elsevier B.V. All rights reserved

Journal of Magnetism and Magnetic Materials 323[14], 1890-1894. 2011.

[P074-11] "Dynamics of a Bose-Einstein condensate in a symmetric triple-well trap"

Viscondi, T. F. and Furuya, K.

We present a complete analysis of the dynamics of a Bose-Einstein condensate trapped in a symmetric triple-well potential. Our classical analogue treatment, based on a time-dependent variational method using SU(3) coherent states, includes the parameter dependence analysis of the equilibrium points and their local stability, which is closely related to the condensate collective behaviour. We also consider the effects of off-site interactions, and how these 'cross-collisions' may become relevant for a large number of trapped bosons. Even in the presence of cross-collisional terms, the model still features an twin-condensate defining characteristics only partially, thus breaking the invariance of the associated quantum subspace.

Moreover, the periodic geometry of the trapping potential allowed us to investigate the dynamics of finite angular momentum collective excitations, which can be suppressed by the emergence of chaos. Finally, using the generalized purity associated with the su(3) algebra, we were able to quantify the dynamical classicality of a quantum evolved system, as compared to the corresponding classical trajectory

Journal of Physics A-Mathematical and Theoretical 44[17]. 175301. 2011.

[P075-11] "Electron inertia effects on the planar plasma sheath problem"

Duarte, V. N. and Clemente, R. A.

The steady one-dimensional planar plasma sheath problem, originally considered by Tonks and Langmuir, is revisited. Assuming continuously generated free-falling ions and isothermal electrons and taking into account electron inertia, it is possible to describe the problem in terms of three coupled integro-differential equations that can be numerically integrated. The inclusion of electron inertia in the model allows us to obtain the value of the plasma floating potential as resulting from an electron density discontinuity at the walls, where the electrons attain sound velocity and the electric potential is continuous. Results from numerical computation are presented in terms of plots for densities, electric potential, and particles velocities. Comparison with results from literature, corresponding to electron Maxwell-Boltzmann distribution (neglecting electron inertia), is also shown. (C) 2011 American Institute of Physics. [doi: 10.1063/1.3581081]

Physics of Plasmas 18[4]. 043504. 2011.

[P076-11] "Enhanced Surface Potential Variation on Nanoprotrusions of GaN Microbelt As a Probe for Humidity Sensing"

Sahoo, P., Oliveira, D. S., Cotta, M. A., Dash, S. D. S., Tyagi, A. K., and Raj, B.

Surface potential (SP) using Kelvin probe microscopy is employed, as a measure to sense humidity, exploiting localized nanoprotrusions of freestanding GaN microbelts. These belts with distinct nanofeatures are grown using chemical vapor deposition technique in the vapor-solid process. The variation of SP value is associated with the surface charge accumulation. Pronounced enhancement of the SP variation is found to arise from the localized inhomogeneity on the nanoprotrusions of microbelt. Role of oxygen-related native defect complexes is also discussed for the observed SP variation with humidity. Furthermore, the rough surface of belts favors a high level of defects on the surface and appears more sensitive to moisture level in atmosphere. Hence attention is essential for any sensing application of chemical species using GaN. A dissociative path way for the reaction mechanism of water molecules on GaN surfaces has been predicted

Journal of Physical Chemistry C 115[13], 5863-5867. 2011.

[P077-11] "Fission track and U-Pb in situ dating applied to detrital zircon from the Vale do Rio do Peixe Formation, Bauru Group, Brazil"

Dias, A. N. C., Tello, C. A. S., Chemale, F., de Godoy, M. C. T. F., Guadagnin, F., Iunes, P. J., Soares, C. J., Osorio, A. M. A., and Bruckmann, M. P.

Combined methods of fission track (FTM) and U-Pb in situ zircon dating were applied to sedimentary samples from the Vale do Rio do Peixe Formation, Bauru Basin, Brazil. Detrital zircons of nine samples were determined by the FTM, and the obtained ages varied from 239 Ma-825 Ma, which can be grouped into four main populations as the 230-300 Ma, 460-490 Ma, 500-650 Ma and 696-825 Ma groups. The U-Pb data show two clear source areas: the Early Paleozoic to Neoproterozoic zircons, ranging from 445 +/- 14 to 708 +/- 18 Ma, and the Paleoproterozoic zircons, ranging from 1879 +/- 23 to 2085 +/- 27 Ma. Subordinate occurrences of Early Neoproterozoic to Mesoproterozoic zircons (836 +/- 15 and 1780 +/- 38 Ma) were identified. The combined information allows us to characterize Early Brazilian, Brazilian and Rhyacian material as the main source for the zircons, which are areas situated to west of the Bauru Basin (e.g., Goias Massif) that have been incorporated into the sedimentary cycles in the Phanerozoic (mainly in the Parana Basin). FT zircon ages reflect the main denudation processes of the South American Plate from Neoproterozoic to Early Triassic as those related to orogenic cycles of Early Brazilian, Brazilian, Famatinian/Cuyanian and Gondwanide. (C) 2011 Elsevier Ltd. All rights reserved

Journal of South American Earth Sciences 31[2-3], 298-305. 2011.

[P078-11] "High p(T) nonphotonic electron production in p plus p collisions at root s=200 GeV"

Agakishiev, H., Aggarwal, M. M., Ahammed, Z., Alakhverdyants, A. V., Alekseev, I., Alford, J., Anderson, B. D., Anson, C. D., Arkhipkin, D., Averichev, G. S., Balewski, J., Beavis, D. R., Behera, N. K., Bellwied, R., Betancourt, M. J., et all

We present the measurement of nonphotonic electron production at high transverse momentum (p(T) > 2.5 GeV/c) in p + p collisions at root s = 200 GeV using data recorded during 2005 and 2008 by the STAR experiment at the Relativistic Heavy Ion Collider (RHIC). The measured cross sections from the two runs are consistent with each other despite a large difference in photonic background levels due to different detector configurations. We compare the measured nonphotonic electron cross sections with previously published RHIC data and perturbative quantum chromodynamics calculations. Using the relative contributions of B and D mesons to nonphotonic electrons, we determine the integrated cross sections of electrons (e++e-2/2) at 3 GeV/c < p(T) < 10 GeV/c from bottom and charm meson decays to be [(d sigma((B -> e)+(B -> D -> e))/(dy(e))](ye=0) 4.0 +/- 0.5(stat) +/- 1.1(syst) nb and [(d sigma(D -> e))/(dy(e))](ye=0) = 6.2 +/- 0.7(stat) +/- 1.5(syst) nb, respectively

Physical Review D 83[5]. 052006. 2011.

[P079-11] "Kinetic Effects in InP Nanowire Growth and Stacking Fault Formation: The Role of Interface Roughening"

Chiaramonte, T., Tizei, L. H. G., Ugarte, D., and Cotta, M. A.

InP nanowire polytypic growth was thoroughly studied using electron microscopy techniques as a function of the In precursor flow. The dominant InP crystal structure is wurtzite, and growth parameters determine the density of stacking faults (SF) and zinc blende segments along the nanowires (NWs). Our results show that SF formation in InP NWs cannot be univocally attributed to the droplet supersaturation, if we assume this variable to be proportional to the ex situ In atomic concentration at the catalyst particle. An imbalance between this concentration and the axial growth rate was detected for growth conditions associated with larger SF densities along the NWs, suggesting a different route of precursor incorporation at the triple phase line in that case. The formation of SFs can be further enhanced by varying the In supply during growth and is suppressed for small diameter NWs grown under the same conditions. We attribute the observed behaviors to kinetically driven roughening

of the semiconductor/metal interface. The consequent deformation of the triple phase line increases the probability of a phase change at the growth interface in an effort to reach local minima of system interface and surface energy

Nano Letters 11[5], 1934-1940. 2011.

[P080-11] "Magnetic and structural properties of fcc/hcp bi-crystalline multilayer Co nanowire arrays prepared by controlled electroplating"

Pirota, K. R., Beron, F., Zanchet, D., Rocha, T. C. R., Navas, D., Torrejon, J., Vazquez, M., and Knobel, M.

We report on the structural and magnetic properties of crystalline bi-phase Co nanowires, electrodeposited into the pores of anodized alumina membranes, as a function of their length. Co nanowires present two different coexistent crystalline structures (fcc and hcp) that can be controlled by the time of pulsed electrodeposition. The fcc crystalline phase grows at the early stage and is present at the bottom of all the nanowires, strongly influencing their magnetic behavior. Both structural and magnetic characterizations indicate that the length of the fcc phase is constant at around 260-270 nm. X-ray diffraction measurements revealed a strong preferential orientation (texture) in the (1 0-1 0) direction for the hcp phase, which increases the nanowire length as well as crystalline grain size, degree of orientation, and volume fraction of oriented material. The first-order reversal curve (FORC) method was used to infer both qualitatively and quantitatively the complex magnetization reversal of the nanowires. Under the application of a magnetic field parallel to the wires, the magnetization reversal of each region is clearly distinguishable; the fcc phase creates a high coercive contribution without an interaction field, while the hcp phase presents a smaller coercivity and undergoes a strong antiparallel interaction field from neighboring wires. (C) 2011 American Institute of Physics. [doi:10.1063/1.3553865]

Journal of Applied Physics 109[8]. 083919. 2011.

[P081-11] "Magnetic field dependence of the magnetic susceptibility and the specific heat of the doped plasticized polyaniline (PANI-DB3EPSA)0.5"

Djurado, D., Pron, A., Jacquot, J. F., Travers, J. P., Adriano, C., Vargas, J. M., Pagliuso, P. G., Rettori, C., Lesseux, G. G., Fier, I., and Walmsley, L.

Specific heat, magnetization and electron spin resonance (ESR) data obtained from a self-standing film of the doped plasticized polyaniline (PANI-DB3EPSA)(0.5) are shown. No long range magnetic order has been observed at zero magnetic field, above 2 K. For a magnetic field of 3.3 kOe applied perpendicular to the plane of the film, a clear signature of an induced ordered state can be seen in the specific heat data and ESR also reveals this antiferromagnetic order. An electronic contribution is detected from ESR, magnetization and specific heat; however, for T <= 5 K, the specific heat data show the existence of a gap. Magnetization data also show a low temperature dominant Curie behaviour which cannot be seen from ESR, probably due to a very large linewidth, suggesting short range correlations among spin 1/2 polarons

Journal of Physics-Condensed Matter 23[20]. 206004. 2011.

[P082-11] "Magnetic properties of metastable Gd-Cr alloys"

Rouxinol, F. P., Gadioli, G. Z., Gelamo, R. V., dos Santos, A. O., Cardoso, L. P., Gama, S., and de Moraes, M. A. B.

We report on the magnetization, magnetocaloric effect, magnetic ordering temperatures, saturation magnetic moments and anisotropy of sputter-deposited GdxCr1-x alloys with Gd atomic concentrations, x, ranging from 0.13 to 0.52. The complex magnetic nature of the Gd-Cr films was revealed from the M x H isotherms, which do not show saturation even at an applied field of 70 kOe and a temperature of 2 K and do not exhibit a linear behavior at higher temperatures. For some of the samples, the isotherms were used to determine the isothermal entropy variation as a function of temperature, for a change of 50 kOe in the applied magnetic field. The saturation magnetic moment varies with x and follows the dilution law, implying that the Cr atoms do not contribute to the total moment of the Gd-Cr alloys. Both static magnetization and dynamic susceptibility measurements reveal the existence of a magnetic glassy behavior in the alloys, which occurs below a freezing temperature. The existence of anisotropy at low temperatures for all samples was revealed by their M x H hysteresis loops from which the in-plane coercive fields, H-c, were determined. A monotonical increase in H-c with increasing Gd concentration was observed. (C) 2011 Elsevier B.V. All rights reserved

Journal of Magnetism and Magnetic Materials 323[15], 2005-2011. 2011.

[P083-11] "Manual and semi-automatic quantification of in vivo H-1-MRS data for the classification of human primary brain tumors"

Cuellar-Baena, S., Morais, L. M. T. S., Cendes, F., Faria, A. V., and Castellano, G

In vivo proton magnetic resonance spectroscopy (H-1-MRS) is a technique capable of assessing biochemical content and pathways in normal and pathological tissue. In the brain, H-1-MRS complements the information given by magnetic resonance images. The main goal of the present study was to assess the accuracy of H-1-MRS for the classification of brain tumors in a pilot study comparing results obtained by manual and semi-automatic quantification of metabolites. In vivo single-voxel H-1-MRS was performed in 24 control subjects and 26 patients with brain neoplasms that included meningiomas, high-grade neuroglial tumors and pilocytic astrocytomas. Seven metabolite groups (lactate, lipids, N-acetyl-aspartate, glutamate and glutamine group, total creatine, total choline, myo-inositol) were evaluated in all spectra by two methods: a manual one consisting of integration of manually defined peak areas, and the advanced method for accurate, robust and efficient spectral fitting (AMARES), a semi-automatic quantification method implemented in the jMRUI software. Statistical methods included discriminant analysis and the leave-one-out cross-validation method. Both manual and semi-automatic analyses detected differences in metabolite content between tumor groups and controls (P < 0.005). The classification accuracy obtained with the manual method was 75% for high-grade neuroglial tumors, 55% for meningiomas and 56% for pilocytic astrocytomas, while for the semi-automatic method it was 78, 70, and 98%, respectively. Both methods classified all control subjects correctly. The study demonstrated that H-1-MRS accurately differentiated normal from tumoral brain tissue and confirmed the superiority of the semi-automatic quantification method

Brazilian Journal of Medical and Biological Research 44[4], 345-353. 2011.

[P084-11] "Measurement of the Neutrino Mass Splitting and Flavor Mixing by MINOS"

Adamson, P., Andreopoulos, C., Armstrong, R., Auty, D. J., Ayres, D. S., Backhouse, C., Barr, G., Bishai, M., Blake, A., Bock, G. J., Boehnlein, D. J., et all

Measurements of neutrino oscillations using the disappearance of muon neutrinos from the Fermilab NuMI neutrino beam as observed by the two MINOS detectors are reported. New analysis methods have been applied to an enlarged data sample from an exposure of 7.25 x 10(20) protons on target. A fit to neutrino oscillations yields values of vertical bar Delta m(2)vertical bar = (2.32(-0.08)(+0.12) x 10(-3) eV(2) for the atmospheric mass splitting and sin(2)(2 theta) > 0.90 (90% C.L.) for the mixing angle. Pure neutrino decay and quantum decoherence hypotheses are excluded at 7 and 9 standard deviations, respectively

Physical Review Letters 106[18]. 181801. 2011.

[P085-11] "Nanostructured tantalum nitride films as buffer-layer for carbon nanotube growth"

Jin, C., Delmas, M., Aubert, P., Alvarez, F., Minea, T., Hugon, M. C., and Bouchet-Fabre, B.

Tantalum nitride (TaNx) films are usually used as barriers to the diffusion of copper in the substrate for electronic devices. In the present work, the TaNx coating plays an extra role in the iron catalyzed chemical vapor deposition production of carbon nanotubes (CNT). The CNTs were grown at 850 degrees C on TaNx films prepared by radio frequency magnetron sputtering. The correlation between the CNT morphology and growth rate, and the pristine TaNx film nature, is investigated by comparing the evolution of the nano-composition, roughness and nano-crystallinity of the TaNx films both after annealing and CVD at 850 degrees C. 2011 Published by Elsevier B.V

Thin Solid Films 519[12], 4097-4100. 2011.

[P086-11] "Quantum flavor oscillations extended to the Dirac theory"

Bernardini, A. E., Guzzo, M. M., and Nishi, C. C.

Flavor oscillations by itself and its coupling with chiral oscillations and/or spin-flipping are the most relevant quantum phenomena of neutrino physics. This report deals with the quantum theory of flavor oscillations in vacuum, extended to fermionic particles in the several subtle aspects of the first quantization and second quantization theories. At first, the basic controversies regarding quantum-mechanical derivations of the flavor conversion formulas are reviewed based on the internal wave packet (IWP) framework. In this scenario, the use of the Dirac equation is required for a satisfactory evolution of fermionic mass-eigenstates since in the standard treatment of oscillations the mass-eigenstates are implicitly assumed to be scalars and, consequently, the spinorial form of neutrino wave functions is not included in the calculations. Within first quantized theories, besides flavor oscillations, chiral oscillations automatically appear when we set the dynamic equations for a fermionic Dirac-type particle. It is also observed that there is no constraint between chiral oscillations, when it takes place in vacuum, and the process of spin-flipping related to the helicity quantum number, which does not take place in vacuum. The left-handed chiral nature of created and detected neutrinos can be implemented in the first quantized Dirac theory in presence of mixing; the probability loss due to the changing of initially left-handed neutrinos to the undetected right-handed neutrinos can be obtained in analytic form. These modifications introduce correction factors proportional to m(v)(2)/E-v(2) that are very difficult to be quantified by the current phenomenological analysis. All these effects can also be identified when the non-minimal coupling with an external (electro) magnetic field in the neutrino interacting Lagrangian is taken into account. In the context of a causal relativistic theory of a free particle, one of the two effects should be present in flavor oscillations: (a) rapid oscillations or (b) initial flavor violation. Concerning second quantized approaches, a simple second quantized treatment exhibits a tiny but inevitable initial flavor violation without the possibility of rapid oscillations. Such effect is a consequence of an intrinsically indefinite but approximately well defined neutrino flavor. Within a realistic calculation in pion decay, including the quantum field treatment of the creation process with finite decay width, it is possible to quantify such violation. The violation effects are shown to be much larger than loop induced lepton flavor violation processes, already present in the standard model in the presence of massive neutrinos with mixing. For the implicitly assumed fermionic nature of the Dirac theory, the conclusions of this report lead to lessons concerning flavor mixing, chiral oscillations, interference between positive and negative frequency components of Dirac equation solutions, and the field formulation of quantum oscillations. (C) 2011 WILEY-VCH Verlag GmbH & Co. KGaA, Weinheim

Fortschritte der Physik-Progress of Physics 59[5-6], 372-453. 2011.

[P087-11] "Room Temperature Ferromagnetism in Pure and Cu Doped Zno Nanorods: Role of Copper Or Defects"

Kumar, S., Koo, B. H., Lee, C. G., Gautam, S., Chae, K. H., Sharma, S. K., and Knobel, M.

We report structural, magnetic and electronic structure studies of pure and Cu doped ZnO nanorods with the aim to understand the origin of ferromagnetism. A structural study indicates that all the samples exhibit single phase nature and rules out the formation of secondary phase. NEXAFS measurements reveal that Cu ions exist in Cu2+ state. Magnetic hysteresis loop measurements reflect that the pure and Cu doped ZnO nanorods exhibit room temperature ferromagnetism. The increase in the intensity of green emission in photoluminescence study indicates that defects density increases with Cu doping

Functional Materials Letters 4[1], 17-20. 2011.

[P088-11] "Scaling properties at freeze-out in relativistic heavy-ion collisions"

Aggarwal, M. M., Ahammed, Z., Alakhverdyants, A. V., Alekseev, I., Alford, J., Anderson, B. D., Anson, C. D., Arkhipkin, D., Averichev, G. S., Balewski, J., et all

Identified charged pion, kaon, and proton spectra are used to explore the system size dependence of bulk freeze-out properties in Cu + Cu collisions at root s(NN) = 200 and 62.4 GeV. The data are studied with hydrodynamically motivated blast-wave and statistical model frameworks in order to characterize the freeze-out properties of the system. The dependence of freeze-out parameters on beam energy and collision centrality is discussed. Using the existing results from Au + Au and pp collisions, the dependence of freeze-out parameters on the system size is also explored. This multidimensional systematic study furthers our understanding of the QCD phase diagram revealing the importance of the initial geometrical overlap of the colliding ions. The analysis of Cu + Cu collisions expands the system size dependence studies from Au + Au data with detailed measurements in the smaller system. The systematic trends of the bulk freeze-out properties of charged particles is studied with respect to the total charged particle multiplicity at midrapidity, exploring the influence of initial state effects

Physical Review C 83[3]. 034910. 2011.

[P089-11] "Search for first harmonic modulation in the right ascension distribution of cosmic rays detected at the Pierre Auger Observatory"

We present the results of searches for dipolar-type anisotropies in different energy ranges above 2.5 x 10(17) eV with the surface detector array of the Pierre Auger Observatory, reporting on both the phase and the amplitude measurements of the first harmonic modulation in the right-ascension distribution. Upper limits on the amplitudes are obtained, which provide the most stringent bounds at present, being below 2% at 99% C.L. for EeV energies. We also compare our results to those of previous experiments as well as with some theoretical expectations. (C) 2011 Elsevier B.V. All rights reserved

Astroparticle Physics 34[8], 627-639. 2011.

[P090-11] "Software development of graphical analysis to radioprotection plans"

Viscovini, R. C., Lopes, N. B., and Pereira, D.

In this work we developed a software that calculates the external doses in a plant radioactive, and presented graphically in contour dose (isodoses) using the geometric method. It was created to help the lessons of radioprotection, but can be used to review plans for radioprotection. The software was written for version 6.0 of the application Mathematica (R) from Wolfram Research for the algebraic and numerical calculation, but can be easily translated into Maple (R), Matlab (R) or Delphi (R). To demonstrate its application, this software is used to prepare the plan for radioprotection of a laboratory that uses a gas isotopic laser ((CO2)-C-14)

Revista Brasileira de Ensino de Fisica 33[1]. 1505. 2011.

[P091-1] "Solutions to the restricted three-body problem with variable mass"

Letelier, P. S. and da Silva, T. A.

We look for particular solutions to the restricted three-body problem where the bodies are allowed to either lose or gain mass to or from a static atmosphere. In the case that all the masses are proportional to the same function of time, we find analogous solution to the five stationary solutions of the usual restricted problem of constant masses: the three collinear and the two triangular solutions, but now the relative distance of the bodies changes with time at the same rate. Under some restrictions, there are also coplanar, infinitely remote and ring solutions

Astrophysics and Space Science 332[2], 325-329. 2011.

[P092-11] "Study of roughness evolution and layer stacking faults in short-period atomic layer deposited HfO2/Al2O3 multilayers"

de Pauli, M., Malachias, A., Westfahl, H., Bettini, J., Ramirez, A., Huang, G. S., Mei, Y. F., and Schmidt, O. G.

In this work we study the evolution of roughness in interfaces of HfO2/Al2O3 multilayers by x-ray reflectivity. It was found that, besides the reduced adatom surface mobility during atomic layer deposition, an improvement of the interface quality can be achieved upon the stacking of several layers. Although the low roughness of the initial surface could not be recovered, there was a considerable improvement of surface/interface quality along the deposition process. In particular, variations on the growth temperature were not able to tailor the surface quality, if compared to the stacking process. Finally, transmission electron microscopy analysis has shown that local defects can take place among nearly perfect interfaces. Such effect must be taken into account for nanometer-scale device fabrication. (C) 2011 American Institute of Physics. [doi:10.1063/1.3555624]

Journal of Applied Physics 109[6]. 063524. 2011.

[P093-11] "Study of sodium tellurite glass using the thermally stimulated depolarization current technique (TSDC)"

Giehl, J. M., Pontuschka, W. M., Barbosa, L. C., Blak, A. R., Navarro, M., and Da Costa, Z. M.

In order to have a better understanding of the role of the structure and the defects involved in the polarization processes in an 85TeO(2)-15Na(2)O mol% glass, we used the thermally stimulated depolarization currents (TSDC technique). The TSDC of the non-irradiated sample presented a strong negative peak of current at the temperature of 340 K, preceded by a relatively weak positive peak at about 300 K. after different d.c. voltages of 1200, 1500 and 2000 V were applied. No response was obtained with 1000 V. but the peak intensity increased considerably for voltages above 1200 V. After gamma-irradiation of 25 and 50 KGy doses, a depolarization of the negative peak was observed in the sample submitted to 25 KGy, whereas for the sample irradiated with 50 KGy, six TSDC peaks appeared at regular intervals of 5 KGy, in the temperature range of 100 and 300 K. Crown Copyright (C) 2010 Published by Elsevier B.V. All rights reserved

Journal of Non-Crystalline Solids 357[6-7], 1582-1586. 2011.

[P094-11] "Studying nanotoxic effects of CdTe quantum dots in Trypanosoma cruzi"

Vieira, C. S., Almeida, D. B., de Thomaz, A. A., Menna-Barreto, R. F. S., dos Santos-Mallet, J. R., Cesar, C. L., Gomes, S. A. O., and Feder, D.

Semiconductor nanoparticles, such as quantum dots (QDs), were used to carry out experiments in vivo and ex vivo with Trypanosoma cruzi. However, questions have been raised regarding the nano toxicity of QDs in living cells, microorganisms, tissues and whole animals. The objective of this paper was to conduct a QD nanotoxicity study on living T. cruzi protozoa using analytical methods. This was accomplished using in vitro experiments to test the interference of the QDs on parasite development, morphology and viability. Our results show that after 72 h, a 200 mu M cadmium telluride (CdTe) QD solution induced important morphological alterations in T. cruzi, such as DNA damage, plasma membrane blebbing and mitochondrial swelling. Flow cytometry assays showed no damage to the plasma membrane when incubated with 200 mu M CdTe QDs for up to 72 h (propidium iodide cells), giving no evidence of classical necrosis. Parasites incubated with 2 mu M CdTe QDs still proliferated after seven days. In summary, a low concentration of CdTe QDs (2 mu M) is optimal for bioimaging, whereas a high concentration (200 mu M CdTe) could be toxic to cells. Taken together, our data indicate that 2 mu M QD can be used for the successful long-term study of the parasite-vector interaction in real time

Memorias do Instituto Oswaldo Cruz 106[2], 158-165. 2011.

[P095-11] "Synthesis and ageing effect in FeO nanoparticles: Transformation to core-shell FeO/Fe3O4 and their magnetic characterization"

Sharma, S. K., Vargas, J. M., Pirota, K. R., Kumar, S., Lee, C. G., and Knobel, M.

This paper reports the magnetic properties of partially oxidized FeO nanoparticles (NPs) prepared using thermal decomposition of iron acetylacetonate at high temperature. X-ray diffraction (XRD) analysis confirmed that the resulting NPs comprise a mixture of wustite and magnetite phases, confirmed using high

resolution transmission electron microscopy (HR-TEM) and selected area electron diffraction (SAED) pattern. Alternatively, below 200 K, a large exchange bias field has been observed in field cooled mode whose magnitude increases with the decrease in measuring temperature attaining a maximum value of similar to 2.3 kOe at 2K accompanied by coercivity enhancement (similar to 3.4 kOe) and high field of irreversibility (> 50 kOe). The results are discussed taking into account the role of interface exchange coupling on the macroscopic magnetic properties of the nanoparticles. (C) 2011 Elsevier B.V. All rights reserved

Journal of Alloys and Compounds 509[22], 6414-6417. 2011.

[P096-11] "Synthesis of Ag-CoFe2O4 dimer colloidal nanoparticles and enhancement of their magnetic response"

Sharma, S. K., Lopes, G., Vargas, J. M., Socolovsky, L. M., Pirota, K. R., and Knobel, M.

This paper reports the structural and magnetic properties of Ag-CoFe2O4 colloidal dimer nanoparticles (NPs) synthesized using a two-step solution-phase route. Ag NPs were used as seeds to grow Ag-CoFe2O4 dimer NPs using thermal decomposition of metallic precursor. By means of temperature and field dependent dc magnetization measurements, it is found that the silver due to its interface with CoFe2O4 particles leads to thermal stabilization of the dimer NPs superior as compared to CoFe2O4 alone. Our results show enhancement of the magnetic anisotropy and a large coercivity at 2 K for dimer NPs, which could be ascribed to interface effect between Ag and CoFe2O4 components and the related structural defects. (C) 2011 American Institute of Physics. [doi:10.1063/1.3556771]

Journal of Applied Physics 109[7]. 2011.

[P097-11] "Temperature effects on the occurrence of long interatomic distances in atomic chains formed from stretched gold nanowires"

Lagos, M. J., Autreto, P. A. S., Legoas, S. B., Sato, F., Rodrigues, V., Galvao, D. S., and Ugarte, D.

The origin of long interatomic distances in suspended gold atomic chains formed from stretched nanowires remains the object of debate despite the large amount of theoretical and experimental work. Here, we report new atomic resolution electron microscopy observations acquired at room and liquid-nitrogen temperatures and theoretical results from ab initio quantum molecular dynamics on chain formation and stability. These new data are suggestive that the long distances are due to contamination by carbon atoms originating from the decomposition of adsorbed hydrocarbon molecules

Nanotechnology 22[9]. 095705. 2011.

[P098-11] "The influence of spontaneous and field-induced spin reorientation transitions on the magnetocaloric properties of HoZn and ErZn"

de Sousa, V. S. R., von Ranke, P. J., and Gandra, F. C. G.

We report a theoretical investigation on the magnetocaloric properties of the cubic CsCl-type HoZn and ErZn compounds. Several anomalies in the magnetocaloric quantities, Delta S-T and Delta T-S, are observed due to spontaneous and/or field-induced spin reorientation transitions in these compounds. In HoZn, a discontinuity in the isothermal entropy change and in the adiabatic temperature change around T-1 = 23 K is ascribed to the spontaneous reorientation transition. Under a magnetic field variation from 0 up to 2 T in the < 110 > and < 100 > directions, an almost table-like behavior in Delta S-T is predicted between T-1 and T-SR1. The peak around the ferromagnetic-paramagnetic transition temperature in the magnetocaloric quantities shows a dependence on the direction of the applied field. For mu(0)Delta H = 2 T, it reaches 11.9 J/kg K (magnetic field along the < 111 > direction) and 7.9 J/kg K (magnetic field in the < 100 > direction). In ErZn there is also a dependence of Delta S-T and Delta T-S on field direction. From the analysis of the spin reorientations in both compounds we have built spin reorientation diagrams that summarize their temperature and field dependence. Our theoretical approach is based on a model Hamiltonian that includes exchange, crystal field, and quadrupolar interactions. (C) 2011 American Institute of Physics. [doi:10.1063/1.3554725]

Journal of Applied Physics 109[6]. 063904. 2011.

[P099-11] "The role of conditioning film formation and surface chemical changes on Xylella fastidiosa adhesion and biofilm evolution"

Lorite, G. S., Rodrigues, C. M., de Souza, A. A., Kranz, C., Mizaikoff, B., and Cotta, M. A.

Biofilms are complex microbial communities with important biological functions including enhanced resistance against external factors like antimicrobial agents. The formation of a biofilm is known to be strongly dependent on substrate properties including hydrophobicity/hydrophilicity, structure, and roughness. The adsorption of (macro)molecules on the substrate, also known as conditioning film, changes the physicochemical properties of the surface and affects the bacterial adhesion. In this study, we investigate the physicochemical changes caused by Periwinkle wilt (PW) culture medium conditioning film formation on different surfaces (glass and silicon) and their effect on X. fastidiosa biofilm formation. Contact angle measurements have shown that the film formation decreases the surface hydrophilicity degree of both glass and silicon after few hours. Atomic force microscopy (AFM) images show the glass surface roughness is drastically reduced with conditioning film formation. First-layer X. fastidiosa biofilm on glass was observed in the AFM liquid cell after a period of time similar to that determined for the hydrophilicity changes. In addition, attenuation total reflection-Fourier transform infrared (ATR-FTIR) spectroscopy supports the AFM observation, since the PW absorption spectra increases with time showing a stronger contribution from the phosphate groups. Although hydrophobic and rough surfaces are commonly considered to increase bacteria cell attachment, our results suggest that these properties are not as important as the surface functional groups resulting from PW conditioning film formation for X. fastidiosa adhesion and biofilm development. (c) 2011 Elsevier Inc. All rights reserved

Journal of Colloid and Interface Science 359[1], 289-295. 2011.

[P100-11] "Theoretical investigation on the existence of inverse and direct magnetocaloric effect in perovskite EuZrO3"

Alho, B. P., Nobrega, E. P., de Sousa, V. S. R., Carvalho, A. M. G., de Oliveira, N. A., and von Ranke, P. J.

We report on the magnetic and magnetocaloric effect calculations in antiferromagnetic perovskite-type EuZrO3. The theoretical investigation was carried out using a model Hamiltonian including the exchange interactions between nearest-neighbor and next-nearest-neighbor for the antiferromagnetic ideal G-type structure (the tolerance factor for EuZrO3 is t = 0.983, which characterizes a small deformation from an ideal cubic perovskite). The molecular field approximation and Monte Carlo simulation were considered and compared. The calculated magnetic susceptibility is in good agreement with the available experimental data. For

a magnetic field change from zero to 2 T a normal magnetocaloric effect was calculated and for a magnetic field change from zero to 1 T, an inverse magnetocaloric effect was predicted to occur below T = 3.6 K. (C) 2011 American Institute of Physics. [doi:10.1063/1.3582144]

Journal of Applied Physics 109[8]. 083942. 2011.

[P101-11] "Thermoelastic analysis of a silicon surface under x-ray free-electron-laser irradiation (vol 81, 073102, 2010)"

de Castro, A. R. B., Vasconcellos, A. R., and Luzzi, R.

Review of Scientific Instruments 82[4]. 049901. 2011.

[P102-11]"Zero-< n > non-Bragg gap plasmon-polariton modes and omni-reflectance in 1D metamaterial photonic superlattices"

Agudelo-Arango, C., Mejia-Salazar, J. R., Porras-Montenegro, N., Reyes-Gomez, E., and Oliveira, L. E.

A theoretical study of the photonic band structure and transmission spectra for 1D periodic superlattices with an elementary cell composed of two layers of refractive indices n(a) and n(b), which may take on positive as well as negative values, has been performed within the transfer-matrix approach. The dependence on the angle of incidence of the electromagnetic wave for excitation of plasmon-polaritons as well as the properties of the < n > = 0 gap were thoroughly investigated. Results are found for the generalized conditions that must be satisfied by the ratio a/b of the layer widths of metamaterial photonic superlattices, for both transverse electric and transverse magnetic polarizations, in order to have an omnidirectional < n > = 0 gap. The present study indicates new perspectives in the design and development of future optical devices

Journal of Physics-Condensed Matter 23[21]. 215003. 2011.

Abstracta

Instituto de Física
Diretor: Prof. Dr. Daniel Pereira
Universidade Estadual de Campinas - UNICAMP
Cidade Universitária Zeferino Vaz
13083-859 - Campinas - SP - Brasil
e-mail: secdir@ifi.unicamp.br
Fone: 0XX 19 3521-5300

Publicação

Biblioteca do Instituto de Física Gleb Wataghin
http://webbif.ifi.unicamp.br
Diretora Técnica: Sandra Maria Carlos Cartaxo

Elaboração
Antonela Carvalho Ribeiro
antonela@ifi.unicamp.br

Projeto Gráfico
ÍgneaDesign

Impressão
Gráfica Central - Unicamp